

APPLICATION OF MAGNETIC MULTIPLE RESONANCES TO STUDY DEFECTS IN III-V COMPOUNDS

J.-M. SPAETH

University of Paderborn, Fachbereich Physik,
Warburger Str. 100A, D-4790 Paderborn, F.R.G.

The application of optical detection of electron spin resonance (ODESR) and electron nuclear double resonance (ODENDOR) using the microwave and radio frequency-induced changes of the magnetic circular dichroism of the optical absorption (MCD) to study the structure of intrinsic and extrinsic defects in III-V semiconductors is briefly reviewed. Experiments to correlate defect structures (ODESR and ODENDOR), the energy levels and bulk optical properties of the crystals are described as well as a novel method to determine the spin value using magneto-optical techniques. Experiments to investigate defect distributions across semiconductor wafers with spatially resolved MCD and ODESR are shown. First ODESR spectra from a thin hetero-structure GaAs/Al_{1-x}Ga_xAs using the emission technique are also presented.

1. INTRODUCTION

The optical detection of electron spin resonance (ODESR), a double resonance experiment, can be achieved in several ways. The major techniques are those using microwave-induced changes of the magnetic circular dichroism of the optical absorption (MCD) or circular polarisation of the emission (MCPE) or simply the microwave-induced changes of the emission intensity. The latter technique was applied extensively to semiconductors by studying intensity changes of the donor-acceptor pair recombination luminescence¹, but suffers from the disadvantage that due to exchange interactions the ODESR lines are very often broad. Almost no ODENDOR experiments (triple resonances including a radio frequency field), none with resolution of ligand hyperfine (hf) interactions, were reported with this technique. The MCD technique was first used in colour centre research mainly with the object to study excited states of F-centres² or impurity centres³. It was not used as an alternative to conventional ESR or ENDOR in this field for studying the ground states of paramagnetic defects.

In III-V compounds like GaAs, GaP or InP, conventional ESR and ENDOR experiments were only of moderate success due to the fact that the ESR lines are usually very

broad because of the strong ligand hf interactions with P, Ga and As atoms and because of the rather low defect concentrations of usually approx. 10^{16}cm^{-3} or less. Therefore, magnetic resonance was far less successful there compared to Si or the II-VI compounds. It was only fairly recently that it was shown that the MCD technique to measure ESR and ENDOR of the ground state of defects in III-V compounds works very well indeed with high sensitivity for both ESR and ENDOR and comparable resolution power for ENDOR as known from conventional ENDOR^{4,5}.

In semiconductors not only the knowledge of defect structures is important, but also the knowledge of the energy levels in the band gap for the electrical crystal properties and the optical properties of defects for application in opto-electronics. The measurement of ODESR/ODENDOR excitation spectra yield the correlation between bulk properties and defect structure information from ESR/ENDOR spectra. For the application of semiconductors like semi-insulating (s.i.) GaAs as substrate material for very large scale integration in microelectronics it is important to study the homogeneity of defect distributions across the semiconductor wafer. Both the MCD technique and emission technique have potential for such investigations. First experiments of this kind were done in GaAs using the MCD technique. Finally the magneto-optical properties of the absorption band for paramagnetic defects can be used to determine the spin of a defect (and thus often its charge state), which is usually very difficult from ESR spectra alone if there are not fine structure splittings resolved.

In this paper recent experiments of the Paderborn group using the MCD-technique to study intrinsic and extrinsic defects in GaAs and GaP are briefly reviewed. First applications of the emission technique to study defects in thin III-V layers are also reported.

2. ODESR AND ODENDOR OF INTRINSIC DEFECTS IN GaAs

In Fig. 1 the basic idea of the MCD method is schematically illustrated for the simplification of an "atomic" optical s-p transition. The allowed optical absorption transitions for right and left polarised light are indicated along with the relative matrix elements. The absorption for both polarisations are split in energy by the spin orbit splitting of the excited state. If this splitting is smaller compared to the phonon width of the absorption bands, the measurement of the MCD as a function of energy yields a derivative structure. If the absorption comes from a Kramers doublet with $S = 1/2$ the MCD is given by²

$$\text{MCD} = \frac{d}{4} (\alpha^+ - \alpha^-) = \frac{1}{2} \alpha_0 d \frac{\sigma^+ - \sigma^-}{\sigma^+ + \sigma^-} \frac{n_+ - n_-}{n_+ + n_-} \quad (1)$$

σ^+ and σ^- are the absorption constants for right and left circular polarised light, α_0 the absorption constant for unpolarised light, σ^+ and σ^- are the cross sections for both polarisations and n_+ and n_- are the occupation numbers of the $m_s = \pm 1/2$ states. d is the crystal thickness.

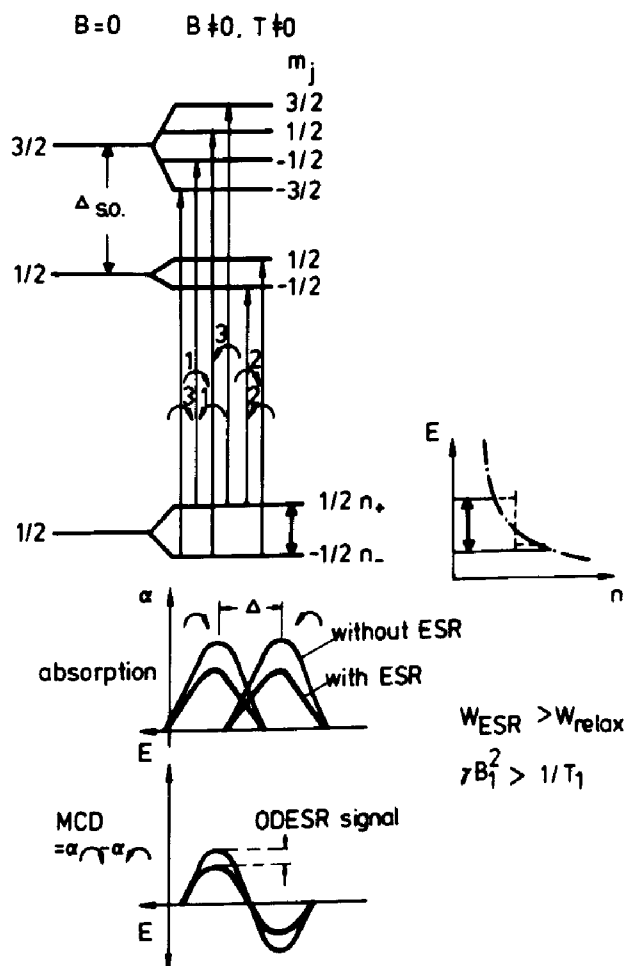


FIGURE 1 Simple "atomic" model to explain the magnetic circular dichroism (MCD) of the absorption and its microwave-induced decrease to detect ESR transitions

The occupation difference $n_+ - n_-$ can be decreased by a microwave transition provided that the microwave transition rate is of the order or larger than the spin lattice relaxation rate $1/T_1$. Such an ESR transition then results in a decrease of the MCD, which is

monitored. The occupation difference ($n_+ - n_-$) depends on the magnetic field and temperature. For $S = 1/2$ one obtains

$$\text{MCD} \propto \tanh\left(\frac{g_e \beta B_0}{2kT}\right) \quad (2)$$

Measurements of the field and temperature dependence of the MCD establishes whether the defect ground state is paramagnetic or diamagnetic. In the latter case the MCD depends only on the magnetic field B_0 , not on the temperature. Recently, the diamagnetic MCD bands of C and Zn acceptors in GaAs in a diamagnetic charge state could be observed⁶.

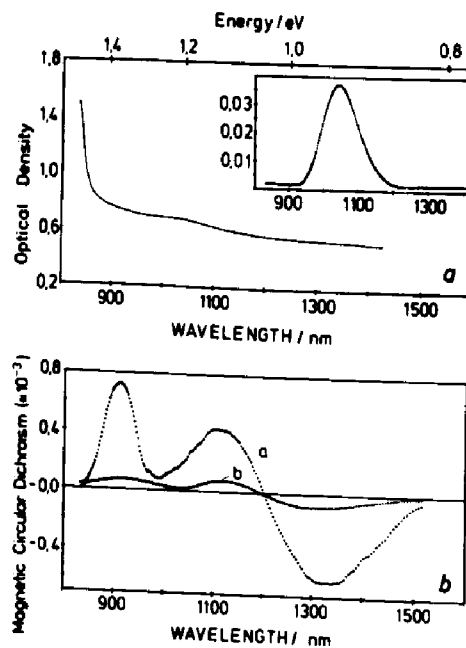


FIGURE 2 Upper half: Optical absorption of "as-grown" semi-insulating GaAs at 1.4 K (crystal thickness 0.3 mm). Lower half: curve a: Magnetic circular dichroism (MCD) of the same sample. $T = 4.2$ K, $B = 2$ T. curve b: Excitation spectrum of the ODESr lines of the EL2^+ defects (MCD tagged by the EL2^+ ESR lines). After /4/.

Fig. 2 shows the optical absorption (Fig. 2a) and the MCD (Fig. 2b) of "as-grown" undoped GaAs, which was grown with the LEC (liquid encapsulated Czochralski) method. Such material is semi-insulating (with high resistivity) due to an intrinsic double donor, which has an energy level at mid gap ($E_v + 0.74$ eV) and one (for the singly ionised charge state) at ($E_v + 0.52$ eV). It was named "EL2" defect and ascribed for a long time to As antisite defects, i.e. As atoms occupying Ga-vacancy sites (As_{Ga})⁷. The mid gap EL2 defect is diamagnetic, the

singly ionised EL2 is paramagnetic. In the absorption below the gap energy of 1.52 eV there is only a very weak band at 1.18 eV due to an intracenter transition of the diamagnetic EL2 defect. The MCD, however, reveals the existence of further intracenter absorption bands due to paramagnetic defects, which turned out to be due to the singly ionised EL2 defect^{4,5,8}. In the direct measurement their weak optical absorption is not detected.

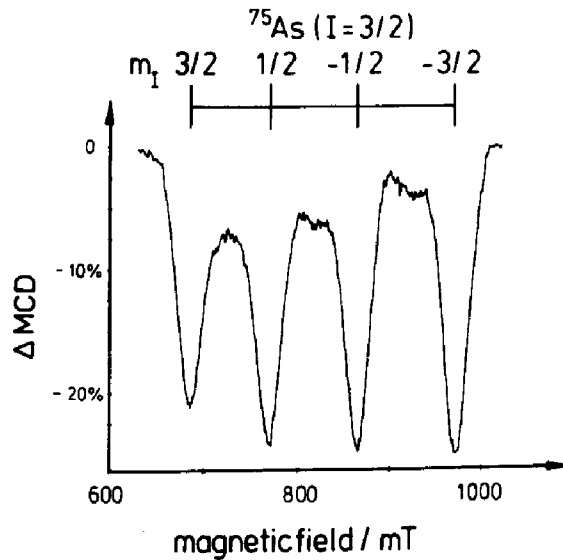


FIGURE 3 Optically detected ESR spectrum of $EL2^+$ defects in s.i. "as-grown" GaAs as microwave-induced decrease of the MCD of the absorption measured at $\lambda = 1350$ nm, $B_0 // \langle 100 \rangle$, $T = 1.5$ K, $\nu_{ESR} = 24$ GHz. After /4/.

When measuring the ODESr in this MCD, e.g. at 1350 nm, the spectrum of Fig. 3 is observed. The quadruplet is due to the hf interaction with a ^{75}As nucleus ($I = 3/2$). The conventional ESR of this defect in as-grown GaAs is very weak, the signal to noise ratio is of the order 2-4 (concentration approx. 10^{16} cm^{-3}). In ODESr there is a gain in signal to noise ratio of about 2 orders of magnitude⁴. From the ESR spectrum the defect structure cannot be inferred since no ligand hf interactions are resolved. In fact, several different MCD spectra were observed in GaAs in which within experimental error identical quadruplet ESR spectra were measured. Such spectra were observed in electron irradiated n- or p-type GaAs and after special heat treatment of s.i. GaAs⁸. If the MCD is different, then the defect structure must be different. The quadruplet splitting of the ESR spectrum reflects only the spin density of the unpaired electron at the ^{75}As nucleus, which for the different As-related defects is the same within experimental precision.

To determine the defect structure one must resolve the ligand- or super-hf interaction by ENDOR, which can be done with the MCD technique.

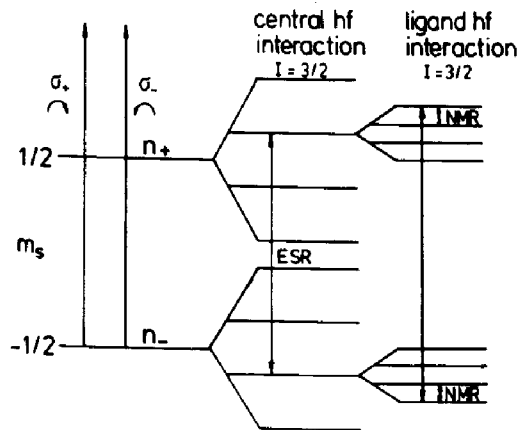


FIGURE 4 Level scheme to illustrate the detection of ENDOR via a rf and microwave-induced decrease of the MCD of the optical absorption.

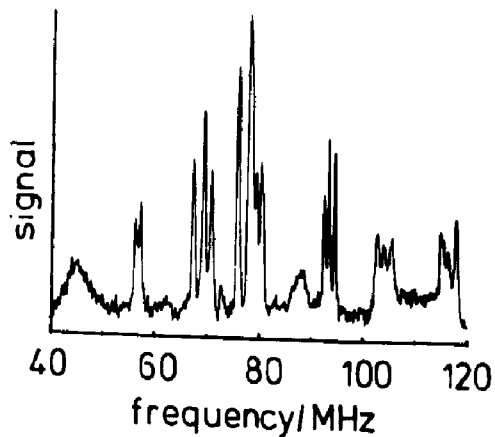


FIGURE 5 Section of the ODENDOR spectrum of the EL2⁺ defects in s.i. "as-grown" GaAs. T = 1.5 K, with B₀ in a (110) plane. The lines are due to ⁷⁵As neighbours of the As_{Ga}⁺, which forms the core of the EL2⁺ defect. After /5/.

Fig. 4 shows the level scheme for the case $S = 1/2$, a central nucleus with $I_c = 3/2$ and one ligand nucleus with $I_l = 3/2$ (e.g. one As neighbour of the As_{Ga} defect). In the experiment one sets the magnetic field onto a particular position of the ODESR line, e.g. into a flank. ESR transitions must obey the selection rule $\Delta m_l = 0, \Delta m_s = \pm 1$. Thus, when measuring the ESR in one of the 4 lines of the $I_c = 3/2$ system, then at most 1/4 of all the spin packets can be

involved, only 1/4 of the MCD can be decreased when saturating the transition. However, if each of the lines is inhomogeneously broadened by further shf interactions, then only a fraction of this decrease should occur, since $\Delta m_{I,a} = 0$ must be obeyed for the ligand I_a . Thus, upon inducing NMR transitions between the nuclear Zeeman levels, one can include more $m_{I,a}$ nuclear substates into the ESR pumping cycle and thus increase the effect of the decrease of the MCD. Therefore, the ENDOR transitions are detected as a further increase of the ODESR signals.

Fig. 5 shows a section of the ODENDOR lines due to the nearest ^{75}As neighbours of the paramagnetic EL2 defect in s.i. as-grown GaAs. The ENDOR lines are sharp and numerous as in conventional ENDOR. The ENDOR signal intensity is mostly several orders of magnitude higher than expected from the simple level scheme model described above. The reason for this favourable observation, which was observed for several different systems both in semiconductors and ionic crystals⁹, is not yet understood.

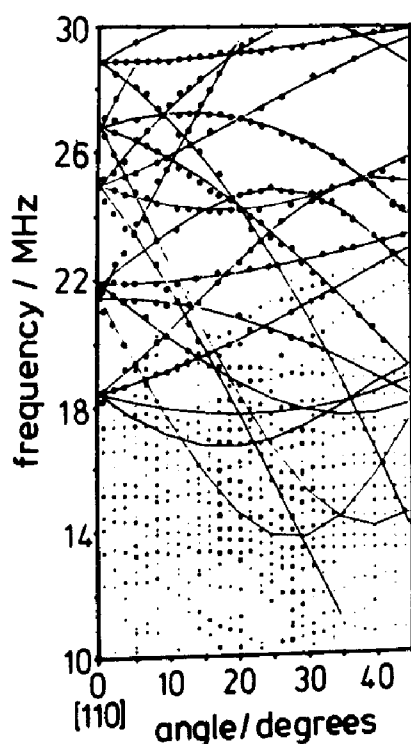


FIGURE 6 Angular dependence of 3rd shell ^{75}As neighbours for rotation in a (110) plane. The solid lines are the calculated angular dependencies for one subshell (IIIa). After/10/.

From the angular dependence the structure model is derived as in conventional ENDOR. Fig. 6 shows the angular dependence of 2 of the subshells observed for the 12 second shell ^{75}As neighbours of the paramagnetic EL2 defects in GaAs¹⁰. The EL2 defect is an arsenic antisite-arsenic interstitial ($\text{As}_{\text{Ga}}-\text{As}_i$) pair defect with C_{3v} symmetry (Fig. 7). The spin density found at the central nucleus and the ligands calculated from a simple LCAO analysis of the shf parameters determined by ODENDOR are indicated in Fig. 7 as % values at each ligand position. It is seen that the As interstitial is part of the total bonding scheme.

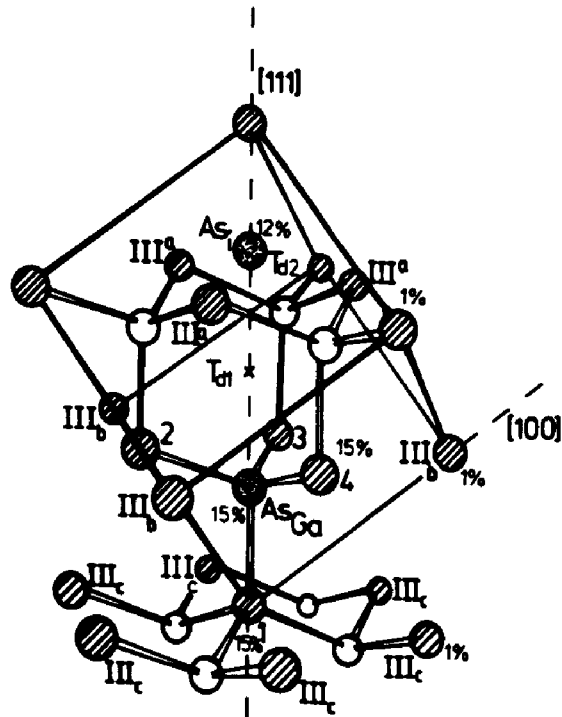


FIGURE 7 Model of the EL2 defect as derived from the ODENDOR experiments. For details see text. After/8/.

3. CORRELATION OF ODESER AND ODENDOR WITH BULK CRYSTAL PROPERTIES

In order to correlate with the energy levels one can perform photo-MCD or photo-ODESR/ODENDOR experiments in samples, where the Fermi level is below the energy level of the paramagnetic defect under investigation. This can be achieved by co-doping with shallow acceptors in GaAs, e.g. by adding Zn. The paramagnetic EL2 level can then be populated by exciting electrons from the valence band into it by illumination of the crystal with a second light

beam of variable photon energy. If this light has the right photon energy to excite electrons into this level, the MCD and the ODESER spectrum appears.

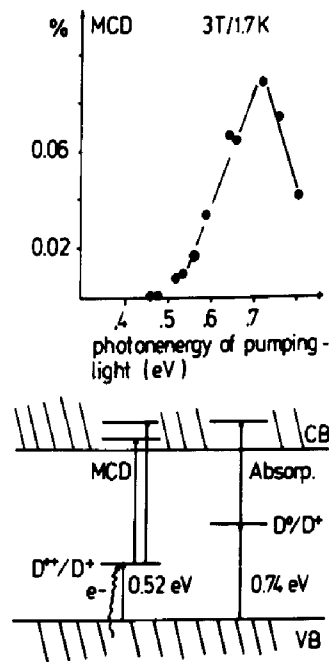


FIGURE 8 Excitation spectrum of the ODESER lines of the $EL2^+$ defects in s.i. "as-grown" GaAs:Zn (p-type). The $EL2^+$ level is occupied by raising the electrons from the valence band as from an exciting photon energy of $h\nu > 0.52$ eV. The diamagnetic $EL2^0$ level is occupied as from $h\nu > 0.74$ eV. The MCD of $EL2^+$ appears above the photon threshold of 0.52 eV and decreases again at 0.74 eV, where $EL2^+$ is transformed into $EL2^0$ by capturing an electron. $T = 1.7$ K, $B = 3$ T. Upper half: experimental results, lower half: level scheme of $EL2^+/EL2^0$. After /8/.

Fig. 8 shows the onset of the MCD of paramagnetic EL2 defects at $(0.52 \pm 0.2$ eV). This is the same level position as determined for this defect by DLTS. Therefore, the the ODESER/ODENDOR spectra described in the last section do indeed belong to the EL2 defect and not to other defects simultaneously present in the crystal. This is further supported by the observation, that at $(0.74 \pm 0.02$ eV) (Fig. 8) the MCD decreases again. Now a second electron is captured to form the diamagnetic EL2 defect. Again, the threshold coincides with the level position determined by DLTS for the mid gap EL2 defect. With the creation of this diamagnetic defect for pumping light with energy exceeding 0.74 eV the EL2 absorption band at 1.18 eV appears. It shows all the typical properties of the EL2 defect like persistent bleaching

and thermal recovery at 140 K^{7,8}. These experiments can also be used to calibrate the MCD, since the band at 1.18 eV was calibrated by DLTS.

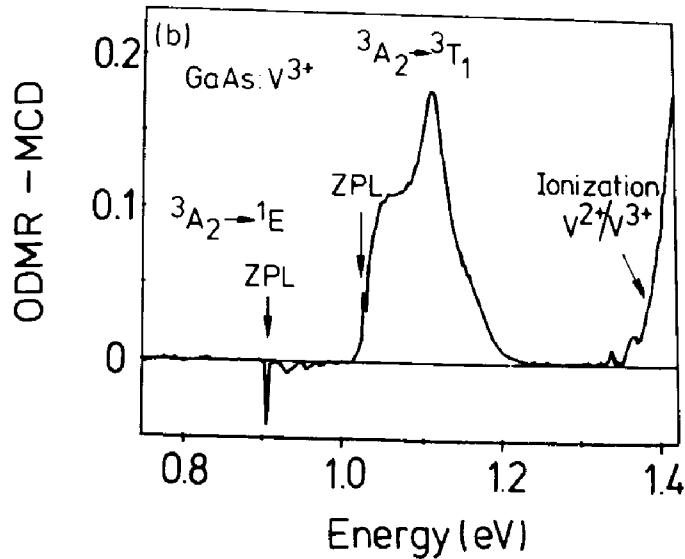


FIGURE 9 Excitation spectrum of the ODESER line of V_{Ga}^{3+} defects in high resistivity GaAs (MCD tagged by ESR). After /12/.

A particular interesting feature of the MCD-ODESR/ODENDOR technique is the possibility to measure a kind of excitation spectrum of ESR or ENDOR lines of specific defect. The schemes of Fig. 1 and 4 apply to all optical transitions of a defect. Therefore, one can set the ESR and ENDOR resonance conditions to a particular ESR or ENDOR line, vary the optical wavelength and monitor the ODESER/ODENDOR signal intensity as microwave (and rf)-induced changes of the MCD¹¹. Thus, from the total MCD of a sample one measures in this way only that part, which belongs to the particularly chosen ESR or ENDOR signal (MCD tagged by ESR/ENDOR). Fig. 2b shows this for $EL2^+$, Fig. 9 shows the MCD tagged by ESR for V_{Ga}^{3+} defects in GaAs. The tagged MCD reveals a rich optical absorption spectrum with several zero phonon lines and phonon replicas, intracenter transitions to Jahn-Teller excited states (between 1.0 and 1.2 eV) and ionising transition at about 1.4 eV into the conduction band¹². The advantage of this method is, that all the transitions belonging to one defect can unambiguously be assigned to this defect via its ESR or ENDOR lines, while in optical spectroscopy alone this is very difficult if different defects are present simultaneously, as is e.g. mostly the case in radiation damage problems and also in semiconductors due to the different charge states of the defects depending on the position of the Fermi level.

It is quite remarkable, that ODESr can also be detected in ionising transitions into either conduction or valence bands and not only in intracenter transitions¹². Apparently, there are continuously defect-induced states resonant with band states, which live long enough to allow optical transitions to occur between states, which contain the spin-orbit splitting and Zeeman properties of the defect. The presence of discrete excited states resonant with the conduction band was experimentally shown by ESR tagging experiments with the ODESr spectra of the P-antisite defects in GaP, where the experimentally found MCD transitions agree qualitatively with theoretical predictions for the occurrence of resonant states in the conduction band¹³.

For low symmetry defects the MCD tagging gives also information on the polarisation of optical transitions by tagging experiments on ESR lines for different defect orientations with respect to the magnetic field¹¹.

4. SPIN DETERMINATION BY MEASURING THE MCD

For $S = 1/2$ the electron spin of a defect can either be determined by a fine structure splitting of the ESR spectrum or by ENDOR. Often, however, there is no fine structure splitting because of symmetry or it is not resolved if too small. With the MCD technique there is an alternative way for the spin determination. The following discussion is precise for an orbital singlet state. If there is orbital degeneracy, the same ideas can be followed, only some possible splittings and spin mixings must be considered¹².

The MCD is composed of a diamagnetic and a paramagnetic term:

$$\text{MCD} = \text{MCD}_{\text{dia}} + \text{MCD}_{\text{para}} \quad (4.1)$$

The diamagnetic term is proportional to the magnetic field B_0 and is usually small compared to the paramagnetic term, which is proportional to the Brillouin function B_S

$$\text{MCD}_{\text{para}} = C \langle S_Z \rangle = C S B_S \quad (4.2)$$

with

$$B_S(\mu) = \frac{1}{2S} \left\{ (2S+1) \coth\left(\frac{2S+1}{2}\mu\right) - \coth\left(\frac{\mu}{2}\right) \right\} \quad (4.3)$$

$$\mu = \frac{g_e \beta_e B_0}{kT} \quad (4.4)$$

Here C is a proportionality constant. As will be seen below C does not enter into the spin determination. B_S depends on B_0 , T , S and the g -factor. For a known g -Factor (from ESR/ODESR) the measurement of B_S as a function of B_0 and T would allow the spin determination. Unfortunately, MCD_{dia} is not known. Since it depends linearly on B_0 , by measuring the total MCD for several magnetic fields (B_1, B_2) and temperatures (T_1, T_2) and forming the ratio:

$$R_{exp} = \frac{MCD(B_1, T_1) - MCD(B_1, T_2)}{MCD(B_2, T_1) - MCD(B_2, T_2)} \quad (4.5)$$

gives

$$R(S) = \frac{BS(S, B_1/T_1) - BS(S, B_1/T_2)}{BS(S, B_2/T_1) - BS(S, B_2/T_2)} \quad (4.6)$$

Equ.(4.6) can be calculated theoretically varying spin S . Thus, the spin of the defect is determined when the conditions $R_{exp} = R(S)$ is fulfilled. Fig. 10 shows this for V_{Ga}^{2+} defects in GaAs, a $3d^3$ configuration, for which a low spin configuration was predicted theoretically. Indeed, this was found¹², as was found $S = 1$ for V^{3+} ($3d^2$), which was also determined in conventional ENDOR experiments^{14,15}.

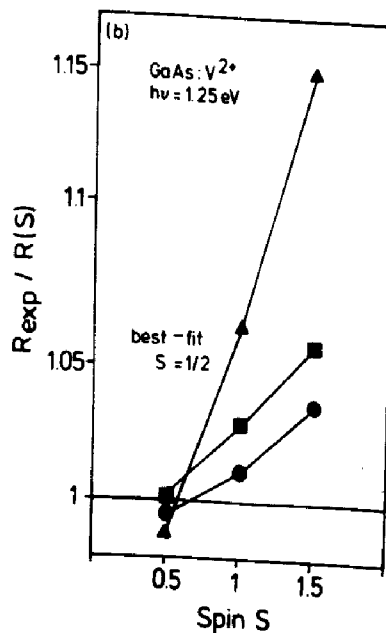


FIGURE 10 Spin determination of V_{Ga}^{2+} centers in GaAs. Ratio of R_{exp} and $R(S)$ as a function of S for V_{Ga}^{3+} measured at 125 eV in high resistivity GaAs:V for the following pairs of magnetic field values: $B_1 = 1$ T, $B_2 = 0.8$ T. $B_1 = 0.8$ T, $B_2 = 0.5$ T. $B_1 = 1.3$ T, $B_2 = 0.5$ T at temperatures $T_1 = 1.65$ K and $T_2 = 4.2$ K. After /12/

5. SPATIALLY RESOLVED MCD MEASUREMENTS

Unlike in NMR spatially resolved conventional ESR measurements are very difficult due to the high magnetic field gradients necessary. With optical detection there is, however, a good possibility for such experiments, where the resolution limit is the optical beam diameter used. Both absorption and emission techniques can be applied.

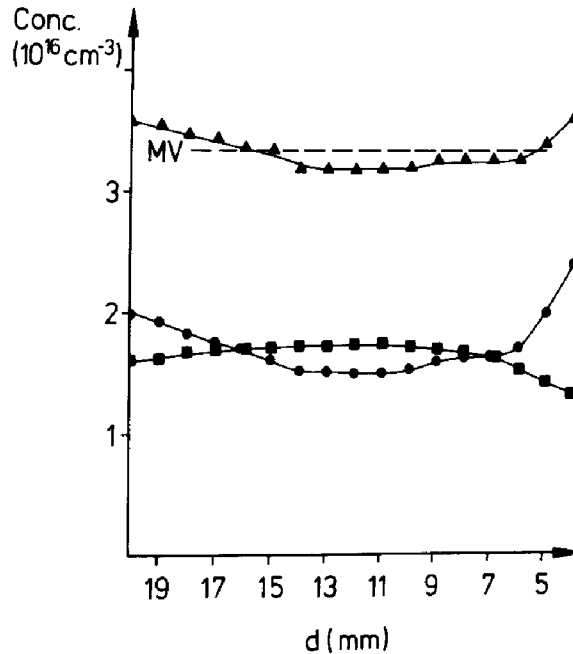


FIGURE 11 Spatially resolved measurement of the IR intracenter absorption band at 1.18 eV of $EL2^0$ and of the MCD at 1350 nm of $EL2^+$ in s.i. "as-grown" GaAs across half a wafer. The distribution of the IR absorption ($EL2^0$) is W-shaped across a wafer, the MCD ($EL2^+$), however, is anticorrelated and M-shaped. The spatial resolution was $0.3 \times 0.3 \text{ mm}^2$. The upper curve: the distribution of the defect in both charge states. After /16/.

Fig. 11 shows a first experiment of this kind using the MCD of paramagnetic EL2 defects in GaAs (at 1350 nm) and the infrared absorption band at $1 \mu\text{m}$ of the midgap diamagnetic EL2 defect to linearly map the concentration of both charge states across half a wafer (thickness $300 \mu\text{m}$, resolution approx. $300 \mu\text{m}$). The two charge states occur almost in anticorrelation. The diamagnetic EL2 defect follows a W-shape, the paramagnetic, ionised EL2 an M-shape, while the defect itself is distributed much more homogeneously compared to the two charge states.

This implies, that the shallow acceptors, which regulate the occupation of $EL2^+$ and $EL2^0$, must exist in a M-shaped distribution. Their nature is probably also intrinsic but not known yet precisely. Possibly, Ga_{As} antisite related defects play a key role in GaAs for the compensation mechanism^{6,16}.

6. ODESr VIA DONOR-ACCEPTOR PAIR RECOMBINATION LUMINESCENCE

The detection of ODESr by observing a microwave-induced change of the luminescence intensity of a donor-acceptor pair recombination was reviewed by Cavenett¹ and is therefore not dealt with in detail here. The major advantage over the MCD technique is the higher sensitivity, which makes this technique the only one if there is only a very small number of defects available for the measurement as in thin layers or very small samples. However, the disadvantage is, that often the lines are very broad due to exchange interactions between donors and acceptors and/or due to short radiation life times. Also indirect paths for the spin dependent transitions make an identification of defects difficult. Very few ENDOR experiments were reported.

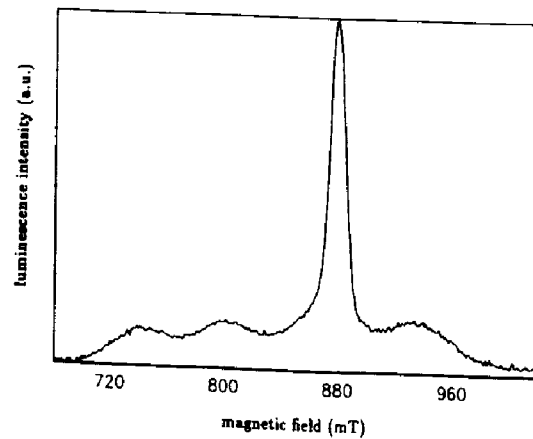


FIGURE 12 ODESr spectrum observed in $Al_{0.99}Ga_{0.18}As/GaAs$ via emission ($\nu = 24$ GHz, 400 mW argon-ion laser excitation, $T = 1.7$ K). The epitaxial $Al_{0.49}Ga_{0.58}As$ layer thickness is $3 \mu m$.

Fig. 12 shows an ODESr spectrum measured with this technique recently in a $GaAs/Al_xGa_{1-x}As$ hetero-structure in the 1.5 μm emission band excited with light of energy exceeding the band gap. The quadruplet spectrum is due to a hf interaction with nuclei of $I =$

$3/2$ and was attributed to Ga interstitials¹⁷, the sharp line with $g = 1.95$ to a donor¹⁸. It seems, however, that both assignments are not yet established enough.

6. CONCLUSIONS

Optical detection of ESR and ENDOR have proved very fruitful for the study of ground states of extrinsic and intrinsic defects in III-V compounds. Of course, if there are enough defects, conventional ENDOR is also a very powerful technique to establish defect structures. Recent examples are the investigation of the Ga-vacancy in GaP¹⁹ and V_{Ga}^{3+} in GaAs and GaP^{14,15}.

REFERENCES:

1. B.C. Cavenett, *Adv. in Physics* **30**, 475 (1983).
2. L.F. Mollenauer and S. Pan, *Phys. Rev. B* **6**, 772 (1972)
3. B.K. Meyer and J.-M. Spaeth, *J. Phys. C: Solid State Phys* **17**, 2253 (1984)
4. B.K. Meyer, J.-M. Spaeth and M. Scheffler, *Phys. Rev. Letts.* **52**, 851 (1984)
5. D.M. Hofmann, B.K. Meyer, F. Lohse and J.-M. Spaeth, *Phys. Rev. Letts.* **53**, 1187 (1984)
6. K. Krambrock, B.K. Meyer and J.-M. Spaeth, 5th Con. on Semi-Insulating III-V Materials, Malmö, Sweden, 1988
7. D.E. Holmes, K.R. Elliott, R.T. Chen and C.G. Kirkpatrick, in: *Semi-Insulating III-V Materials*, ed. by S. Makram-Ebeid, and B. Tuck (Shiva, Nentwich, 1982) p. 19
8. B.K. Meyer, D.M. Hofmann, J.R. Niklas and J.-M. Spaeth, *Phys. Rev. B* **36**, 1332 (1987)
9. M. Fockele, F. Lohse, J.-M. Spaeth and R.H. Bartram, to be published in *J. Phys. C: Solid State Physics* in press and abstract of the 11th Int. Conf. on Defects in Semi-Insulating Crystals, Parma, Italy, 1988
10. D.M. Hofmann, Dissertation Paderborn, 1987
11. F.J. Ahlers, F. Lohse, J.-M. Spaeth and L.F. Mollenauer *Phys. Rev. B* **28**, 1249 (1983)
12. A. Görger, B.K. Meyer, J.-M. Spaeth and A. Hennel, *J. Phys. C: Solid State Phys.*, in press
13. B.K. Meyer and J.-M. Spaeth, *Phys. Rev. B* **32**, 1409 (1985)
14. J. Hage, Dissertation Paderborn, 1987
15. J. Hage, J.R. Niklas and J.-M. Spaeth, to be published
16. M. Heinemann, B.K. Meyer, J.-M. Spaeth and K. Löhnert in: E.R. Weber, ed. *Defect Recognition and Image Processing in III-V Compounds II*, Elsevier Sci. Publ., B.V. Amsterdam 1987
17. T.A. Kennedy and M.G. Spencer, *Phys. Rev. Letts.* **57**, 2690 (1986)
18. E.A. Montie and J.C.M. Henning, *J. Phys. C: Solid State Phys.* **21**, L311 (1988)
19. J. Hage, J.R. Niklas and J.-M. Spaeth, *Mat.Sci. Forum* **10-12**, 259 (1986)